This article was downloaded by:
On: *14 January 2011*
Access details: *Access Details: Free Access*
Publisher *Taylor & Francis*
Informa Ltd Registered in England and Wales Registered Number: 1072954 Registered office: Mortimer House, 37-41 Mortimer Street, London W1T 3JH, UK

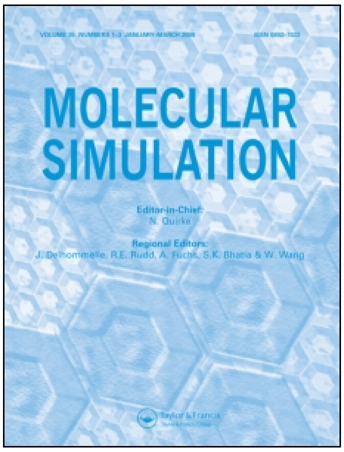

Molecular Simulation
Publication details, including instructions for authors and subscription information:
http://www.informaworld.com/smpp/title~content=t713644482

Influence of polymer structure on adsorption behavior at solid-liquid interface by Monte Carlo simulation

L. Sun[a]; C. Peng[a]; H. Liu[a]; Y. Hu[a]
[a] Lab for Advanced Materials and Department of Chemistry, East China University of Science and Technology, Shanghai, People's Republic of China

To cite this Article Sun, L. , Peng, C. , Liu, H. and Hu, Y.(2007) 'Influence of polymer structure on adsorption behavior at solid-liquid interface by Monte Carlo simulation', Molecular Simulation, 33: 12, 989 — 997

To link to this Article: DOI: 10.1080/08927020701516321

URL: http://dx.doi.org/10.1080/08927020701516321

PLEASE SCROLL DOWN FOR ARTICLE

Full terms and conditions of use: http://www.informaworld.com/terms-and-conditions-of-access.pdf

This article may be used for research, teaching and private study purposes. Any substantial or systematic reproduction, re-distribution, re-selling, loan or sub-licensing, systematic supply or distribution in any form to anyone is expressly forbidden.

The publisher does not give any warranty express or implied or make any representation that the contents will be complete or accurate or up to date. The accuracy of any instructions, formulae and drug doses should be independently verified with primary sources. The publisher shall not be liable for any loss, actions, claims, proceedings, demand or costs or damages whatsoever or howsoever caused arising directly or indirectly in connection with or arising out of the use of this material.

Molecular Simulation, Vol. 33, No. 12, October 2007, 989–997

Influence of polymer structure on adsorption behavior at solid–liquid interface by Monte Carlo simulation

L. SUN, C. PENG, H. LIU* and Y. HU

Lab for Advanced Materials and Department of Chemistry, East China University of Science and Technology, Shanghai 200237,
People's Republic of China

(Received March 2007; in final form June 2007)

Monte Carlo simulations for the adsorption of polymers including random copolymer, homopolymer, diblock copolymer and two kinds of triblock copolymers, respectively, in nonselective solvent at solid–liquid interface have been performed on a simple lattice model. The effect of polymer structure on adsorption properties was examined. In simulations, all polymeric molecules are modeled as self-avoiding linear chains composed of two segments A and B while A is attractive to the surface and B is non-attractive. It was found that for all polymers, the size distribution of various configurations is determined by the linked sequence of segments and the interaction energy between segment and surface. The results of simulation show that the adsorbed amount always increases with increasing bulk concentration but the adsorption layer thickness is mostly dependent on the adsorption energy at a fixed fraction of segments A. On the other hand, diblock copolymer has always the highest surface coverage and adsorbed amount, while random copolymers and homopolymers give generally the smallest surface coverage and adsorbed amount. It is shown that the sequence of polymer chains, i.e. molecular structure, is the most important factor in affecting adsorption properties at the same composition and interaction between segment and surface. The results also show that the adsorption behavior of random copolymers is remarkably different from that of block copolymers, but acting like homopolymer.

Keywords: Random copolymer; Block copolymer; Homopolymer; Surface adsorption; Monte Carlo simulation; Lattice model

Downloaded At: 17:46 14 January 2011

1. Introduction

Polymer adsorption plays an important role in many practical applications, such as colloid stability, adhesion, biology, polymer technology and so on. To understand the mechanism and improve the techniques, it is crucial to obtain the conformation of polymer chains in the vicinity of interface.

Many studies have addressed the adsorption properties of copolymers from experimental techniques [1–4] to theoretical analysis [5–7]. However, it is generally difficult to establish the explicit microstructure of adsorbed layers solely from experimental or theoretical approaches because they were not able to observe various configurations and their distribution directly. On the other hand, this information can be provided intuitively with the aid of computer simulation. In addition, computer simulation can be used to test the reliability of theoretical prediction. As known, a series of works by Monte Carlo (MC) simulations have been reported in the literatures for diblock copolymers [8–16] and triblock copolymers [17–20] as well as random copolymers [21,22].

Although the adsorption behaviours of copolymers have been studied by computer simulation, whose results dispersed in the other literatures without any similarity and difference of these copolymer adsorptions compared systematically. In our previous work, we have studied the adsorption behavior of monodisperse and polydisperse homopolymer [23,24], diblock copolymer [25], symmetrical and asymmetrical triblock copolymer [26–28] at solid–liquid interface by lattice MC simulation. In this work, we extended this approach further to study the adsorption behavior of random copolymers on solid–liquid surface. The importance of this work is to compare different types of polymers by combining with the previous work, and to examine the effect of structure on adsorption properties. The efforts were concentrated on depicting the microstructure of adsorption layers. The profiles of adsorbed segments as tails, loops and trains, as well as the size distributions of these adsorption configurations

---

*Corresponding author. Tel.: +86-21-64252921. Fax:+86-21-64252921. Email: hlliu@ecust.edu.cn

Molecular Simulation
ISSN 0892-7022 print/ISSN 1029-0435 online © 2007 Taylor & Francis
http://www.tandf.co.uk/journals
DOI: 10.1080/08927020701516321

were studied in detail. The macrostructure information such as surface coverage, adsorption amount and adsorption layer thickness were also estimated.

The outline of this paper is as follows: in Section 2, we introduce the simulation techniques. In Section 3, the application of this method to some copolymer systems is described to learn how variations in chain sequence and adsorption energy affect the adsorption properties of polymers from the surface to the bulk. A brief summary of our conclusions is given in Section 4.

2. Simulation method

MC simulation is performed on a cubic lattice in the NVT ensemble. A size of $L_x \times L_y \times L_z = 50 \times 50 \times 50$ was adopted. The simulation box has periodic boundary conditions in the x and y directions. In the z direction, two adsorbing surfaces are located at $z = 0$ and $z = L_z + 1$. All copolymer molecules are modeled as self-avoiding linear chains. Each segment occupies one site and those empty sites are considered to be occupied by solvent molecules S, each of them also occupying one site. The copolymers contain two types of segments: A and B, while the segment A is attractive and segment B is non-attractive to the surface. The values of segment–surface interaction potential are assigned as $\tilde{\varepsilon}_{\mathrm{Aa}}$ and $\tilde{\varepsilon}_{\mathrm{Ba}}$. The segment–surface interaction potential is short-ranged, acting only between the sites on the adsorbing surface and the segments that are on the plane adjacent to the adsorbing surface ($z = 1$ or $z = L_z$). The values of segment–segment and segment–solvent interaction potentials A–A, A–B, B–B, A–S, B–S and S–S are assumed to be zero.

Chain molecules are introduced into the simulation box by using the Rosenbluth–Rosenbluth growth technique [29]. Five types of molecular motion, i.e. Verdier–Stockmayer mode [30] including end-rotation, L-flip and crankshaft motion (or kink jump motion), reptation and the revised Rosenbluth–Rosenbluth growth (configurational-bias sampling) method proposed by Siepmann *et al.* are used. The simulation algorithm was described in detail in our previous papers [23–28].

Despite a great deal of data have been obtained by simulation, in this paper the influence of structure on the adsorption properties is principally discussed by comparing different types of copolymers which are composed of A segment with length of 10 and B segment with length of 20. According to chain sequence, there are four types of copolymers discussed in this paper: diblock copolymer $A_{10}B_{20}$, triblock copolymer $A_5B_{20}A$ and $B_{10}A_{10}B$, random copolymer $(A_{1/3}B_{2/3})_{30}$, respectively, with the same $\tilde{\varepsilon}_{\mathrm{Aa}}$ and $\tilde{\varepsilon}_{\mathrm{Ba}} = 0$. Also an equivalent homopolymer A_{30}^{homo} has been introduced. Thus, we define the effective adsorption energy of one polymer:

$$\tilde{\varepsilon}_{\mathrm{a}}^{\mathrm{polymer}} = f\tilde{\varepsilon}_{\mathrm{Aa}} + (1 - f)\tilde{\varepsilon}_{\mathrm{Ba}} \tag{1}$$

where f is the fraction of segment A in a chain

Obviously, $\tilde{\varepsilon}_{\mathrm{a}}^{\mathrm{polymer}}$ of four copolymers $A_{10}B_{20}$, $A_5B_{20}A$, $B_{10}A_{10}B$, $(A_{1/3}B_{2/3})_{30}$ is the same. Because homopolymer is only composed of segment A, $\tilde{\varepsilon}_{\mathrm{Aa}}$ of A_{30}^{homo} should be decreased to make the adsorption energy of every polymer equal. For example, $\tilde{\varepsilon}_{\mathrm{a}}^{\mathrm{polymer}} = 0.4$ if $\tilde{\varepsilon}_{\mathrm{Ba}} = 0$ and $\tilde{\varepsilon}_{\mathrm{Aa}} = 1.2$ for the copolymers. To ensure $\tilde{\varepsilon}_{\mathrm{a}}^{\mathrm{polymer}}$ of $A_{30}^{\mathrm{homo}} = 0.4$, $\tilde{\varepsilon}_{\mathrm{Aa}}$ must be 0.4, correspondingly.

The number density of chains Φ_c in the system can be calculated as follows:

$$\Phi_c = M/(L_x \times L_y \times L_z) \tag{2}$$

where M is the number of chains introduced into the simulation box. Segments directly adjacent to the surface are regarded as adsorbed segments. Those non-adsorbed chains are called free chains, and segments belong to the free chains are correspondingly called free segments. The segment density or concentration $\rho(z)$ at layer z is defined as the number of segments N_z for both adsorbed chains and free chains in the layer z per surface lattice site. It is calculated by

$$\rho(z) = N_z/(L_x \times L_y) \tag{3}$$

The adsorbed chains usually present in various configurations, which can be generally characterized by trains (sequences in actual contact with the surface), loops (stretches of segments in the solution of which both ends are on the surface), and tails (at the ends of the chain with only one side fixed on the surface). In lattice model, the size of trains configurations can be changed between 1 and r; and r is the length of a chain. The size of tails varies from 1 to $r - 1$, and varies from 2 to $r - 2$ for loops.

The segment density of configuration S along z direction is calculated by

$$\rho(z)_S = N_{Z,S}/(L_x \times L_y) \tag{4}$$

where $N_{Z,\,S}$ is the number of segments in the layer z belong to configuration S (S = tail, train or loop).

There are 50 lattice layers between two surfaces of the simulation box. It is seen from the figures in this work that adsorption layers typically extend up to approximately 10 layers away from the surface. Therefore, the bulk concentration ϕ_b, segment density of the region where the concentration of segments is constant along lattice layers, can be determined by averaging the most intermediate 20 layers, i.e. the layers between 15 and 35.

The adsorption amount Γ is defined as the average number of adsorbed chains' segments per surface lattice site,

$$\Gamma = (N_a \times r)/(L_x \times L_y) \tag{5}$$

where N_a is the number of adsorbed chains with a length r on a surface, $L_x \times L_y$ is the total number of lattice sites on a surface.

The surface coverage θ is defined as the segment density or concentration at layer $z = 1$ or $z = L_z$, i.e. $\theta = \rho(1)$ or $\theta = \rho(L_z)$.

Downloaded At: 17:46 14 January 2011

Downloaded At: 17:46 14 January 2011

We adopted the root-mean-square (RMS) layer thickness employed by Scheutjens and Fleer [31] to determine the adsorption layer thickness in this work:

$$\sigma^2 = \sum_{i=1}^{L} i^2 \rho(i) \Big/ \sum_{i=1}^{L} \rho(i) \tag{6}$$

where i is the consecutive number of layers, $\rho(i)$ is the segment concentration in layer i.

3. Results and discussion

3.1 Density profiles

When $\Phi_c = 0.0048$ and $\tilde{\varepsilon}_a^{\text{polymer}} = 0.4$, the segment density profiles for five systems are depicted in figure 1 for (a) A segments, (b) B segments and (c) total segments. For homopolymer is only compose of segment A, the density profile of segment A is just the total density profile. It could be known from Section 2 that it is $\tilde{\varepsilon}_{\text{Aa}} = 0.4$ for A_{30}^{homo} and $\tilde{\varepsilon}_{\text{Aa}} = 1.2$ for the others when $\tilde{\varepsilon}_a^{\text{polymer}} = 0.4$, thus the property of segment A for homopolymer and copolymers is not the same at all.

Segments A form a thin adsorbed layer directly adjacent to the surface by manifesting a maximum density in the first layer. Obviously, this is because the attractive interaction with surface enhances a preferential adsorption. With the increasing distance from surface, the density of segments A decreases quickly and then increases a little approaching to the bulk value for all the copolymers except random copolymer. The density profile of segment A for random copolymer decreases monotonously, the maximum, but less than any other copolymers, is at $z = 1$ and almost descends straight downwards to the bulk. Figure 1(a) predicts the decreasing order of surface coverage for segment A is $A_{10}B_{20}$, $B_{10}A_{10}B$, $A_5B_{20}A$, $(A_{1/3}B_{2/3})_{30}$. Similar results have also been found in our previous works. However, with the given chain composition and adsorption energy, the segment density of random copolymers in the first layer is the lowest among all the copolymers. In contrast, block copolymers with the same fraction as random copolymer adsorb more strongly. There is a strong preferential adsorption of chains with longer attractive blocks.

Figure 1(b) shows that segment B, expelled by the attractive segment A, exhibits a lower density in the first layer, then increases with the increase distance from the surface and reaches a maximum at several layers away. It can be seen that segment B, although non-attractive, can still be adsorbed onto the surface with small adsorption amount due to chain connectivity. The exact position of the maximum is determined mainly by the position of attractive block located and the length of non-attractive block. It is at the 3rd layer for $B_{10}A_{10}B_{10}$ and $A_5B_{20}A_5$ and the 4th layer for $A_{10}B_{20}$. The result shows, with definite adsorption energy and chain composition, the structure of polymers becomes the dominant factor which affects the density profile of non-absorbed segment.

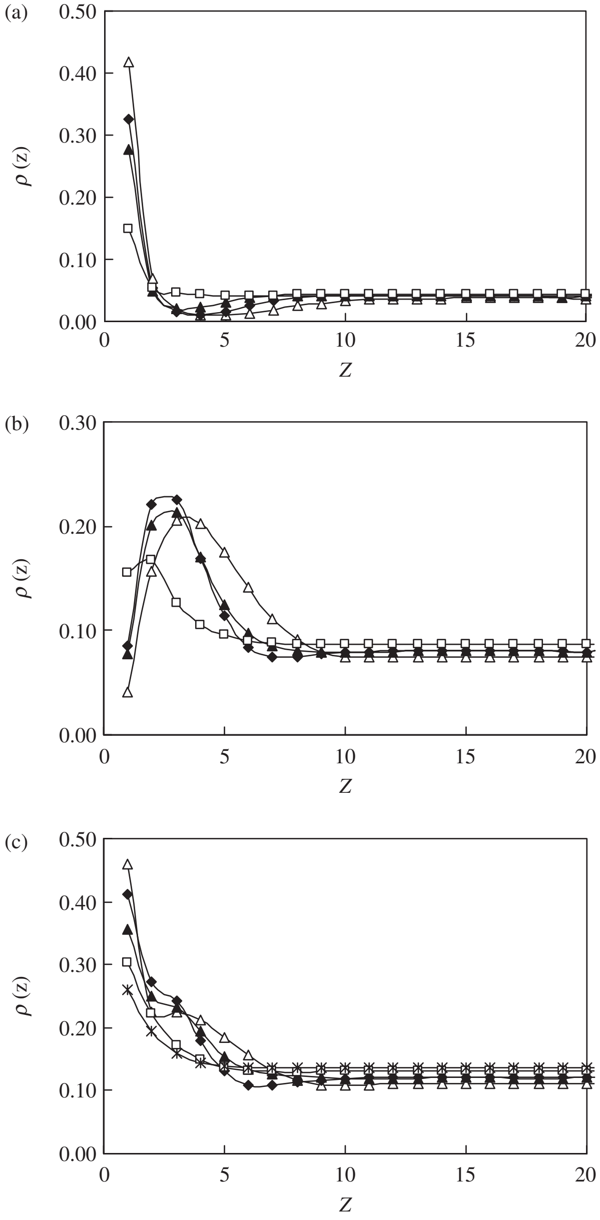

Figure 1. Segment density profiles of segments A (a) and B (b) as well as total segments (c) for five systems when $\Phi_c = 0.0048$ and $\tilde{\varepsilon}_a^{\text{molecule}} = 0.4$. Open triangle: $A_{10}B_{20}$; solid triangle: $A_5B_{20}A_5$; solid diamond: $B_{10}A_{10}B_{10}$; open square: $(A_{1/3}B_{2/3})_{30}$; star: A_{30}^{homo}.

From Figure 1(c), the largest density in the first layer is achieved by $A_{10}B_{20}$, then by $B_{10}A_{10}B_{10}$ and $A_5B_{20}A_5$, and the smallest by $(A_{1/3}B_{2/3})_{30}$ and A_{30}^{homo}, which indicates the surface coverage should show the same sequence, also the similar results were obtained for other copolymers [25,26]. With the increasing distance from the surface, the values of density between $A_{10}B_{20}$ and $A_5B_{20}A_5$ would be exchanged, but $B_{10}A_{10}B_{10}$ is still in the middle. For block copolymers, a plateau is observed at about the second or third layer; however, the density profile of random copolymer is something like that of homopolymer, all decrease monotonously until changeless. The similar phenomena would occur in following results repeatedly.

Downloaded At: 17:46 14 January 2011

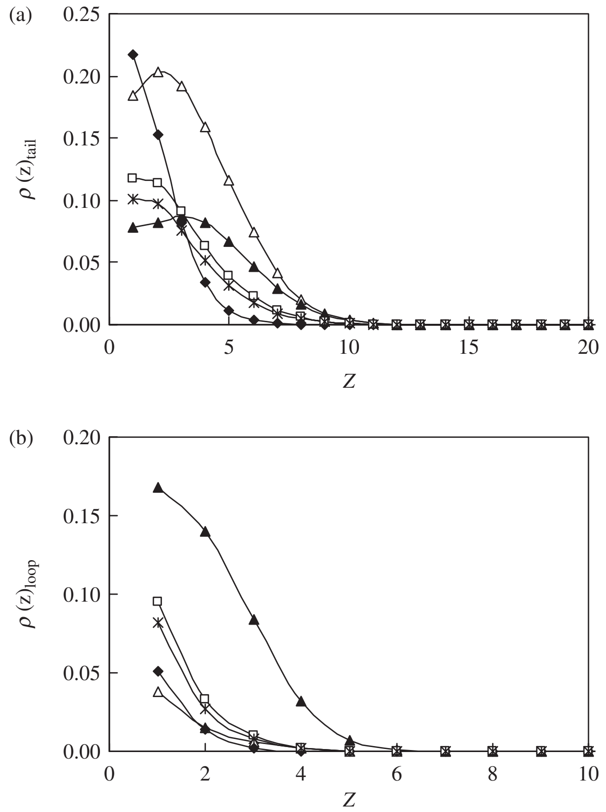

Figure 2. Segment density profiles of tails (a) and loops (b) for five systems when $\Phi_c = 0.0048$ and $\varepsilon_a^{\text{molecule}} = 0.4$. Legends are as in figure 1.

In figure 1, since density profile is the summation of the segments of adsorbed polymer and free segments of unadsorbed polymer, next we will study the effect of the former factor on density profiles solely. Figure 2 shows the segment density profiles of tails (a) and loops (b) for five systems with respect to the distance from the surface when $\Phi_c = 0.0048$ and $\varepsilon_a^{\text{polymer}} = 0.4$.

From this figure, we can see that the variation of polymers has so much tremendous influence on the shape and the relative positions of density profiles for tails and loops. It is shown that the loops are distributed closer to the surface as expected, disappearing at the 6th layer. Nevertheless, the segment density profiles of tails are more dispersed, extending until Z is about the 10th layer. The concentration of tails closed to the surface is much greater than that of loops except for $A_5B_{20}A_5$ as shown in figure 2(a),(b), which implies the important role of tails, especially those tails of non-attractive block B, in determining the adsorption layer thickness of copolymers. This will be discussed in Section 3.5. Also, it seems that the density profiles of tails are more complicated than that of loops.

First, we inspect the segment density profiles of tails in figure 2(a). The maximum of $B_{10}A_{10}B_{10}$ appears at $Z = 1$ then decreases rapidly with the increase distance from the surface. As to $A_5B_{20}A_5$ and $A_{10}B_{20}$, the peak would be reached a little away from the surface and then approaches to zero gradually, which corresponds to the case that one end of terminal copolymer chain is absorbed on the surface and the other end is not adsorbed. However, the appearance of peak means that tails prefer to entangle with each other rather than stretch extending into the bulk. For random copolymer and homopolymer, the change of density along the z direction is mild which decreases monotonically to the bulk value after the maximum, also the profile and the trend are similar.

Second, we inspect the loops which seem to be simpler comparing with the tails. It could be seen from figure 2(b) that the density profiles of loops always have peaks at $Z = 1$ for all the polymers, which implies that the smaller loops are most likely to exist in the adsorption layers. Then the density profiles of loops monotonically decrease along Z. The density drops very fast as Z increases for most of polymers except that of loops for two-terminal copolymers $A_5B_{20}A_5$ exhibit a smaller downtrend along the layers. It is mainly because the length of non-attractive block B is longer which is likely to form bigger size of loops as shown in figure 5(b). We also find for random copolymer and homopolymer, the density distributions of loops, wherever from the shape or the trend, are all the same roughly. In a word, the structure of copolymers is the dominant factor in determining segment density distribution when chain composition and adsorption energy are confirmed. However, the simulation results show that the total density for random copolymers, as well as the density of tails and loops, it seems to be replaced by a corresponding homopolymer.

3.2 *Size distributions of various configurations of all adsorbed copolymers*

The density profiles presented above represent statistical microstructure information of adsorbed layers concerning different kinds of configurations irrespective of detailed sizes of those configurations. This section continues the microstructure discussion and focuses on the size distributions of various adsorption configurations.

The size distribution of tails is the most complicated shown in figure 3(a),(b) (Notice, n in x-axis is the size of various configurations.) When the adsorption energy is smaller, the size distribution profiles of tails obtained from MC simulation are multimodal as shown in figure 3(a). The peak of $B_{10}A_{10}B_{10}$ appears at $n = 10$ and that of $A_{10}B_{20}$ is at $n = 20$, which just equal to the length of non-attractive block B in the end of chains, while $A_5B_{20}A_5$ is at $n = 25$ corresponding to the case that only one of chain ends is adsorbed. In other words, it means that one of the two A blocks is fully adsorbed with leaving the block B and the other block A in the bulk as a tail, 25 is just the sum of block B and one block A. From figure 3(b), we also can see that with the increase of $\tilde{\varepsilon}_{Aa}$, not only the height of the first characteristic peak increases, but also the peak becomes sharper, indicating that more segments A are adsorbed and the non-attractive segments in tail tend to become more monodisperse. Homopolymer and random copolymer have no characteristic peak depending on the structure of polymer itself completely. Another peak of the polymers all appears at $n = 1$, mainly coming from the contribution of segment A, especially which is smaller peak for $B_{10}A_{10}B_{10}$ but

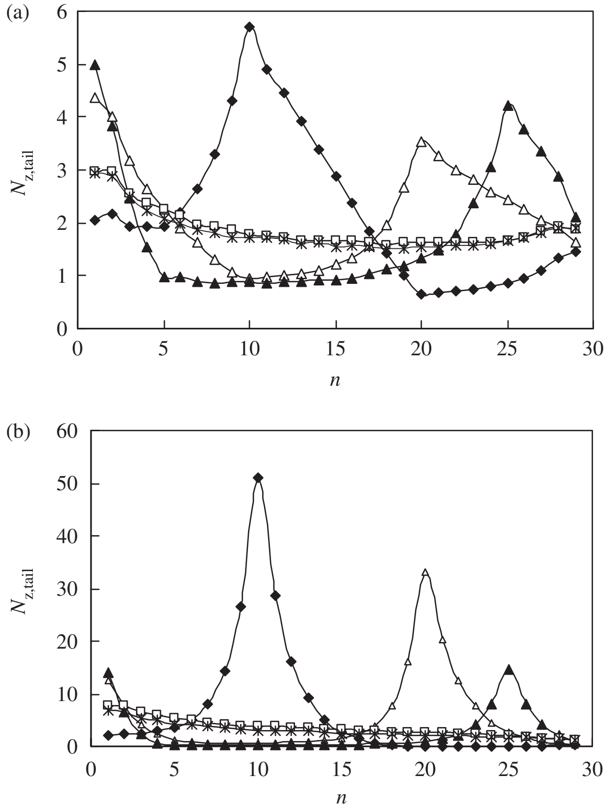

Figure 3. Size distributions of tail configurations for five systems with $\Phi_c = 0.0048$ when $\tilde{\varepsilon}_a^{\mathrm{molecule}} = 0.133$ (a) and $\tilde{\varepsilon}_a^{\mathrm{molecule}} = 0.4$ (b). Legends are as in figure 1.

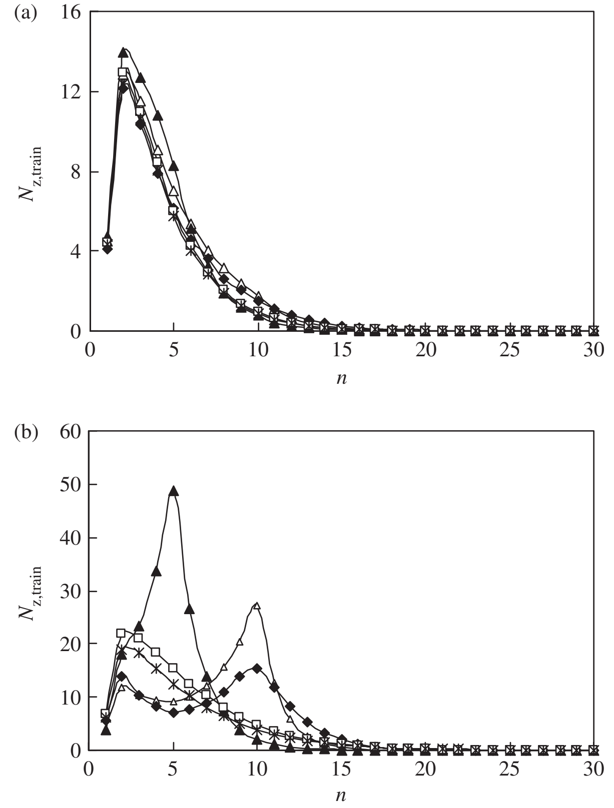

Figure 4. Size distributions of train configurations for five systems with $\Phi_c = 0.0048$ when $\tilde{\varepsilon}_a^{\mathrm{molecule}} = 0.133$ (a) and $\tilde{\varepsilon}_a^{\mathrm{molecule}} = 0.4$ (b). Legends are as in figure 1.

higher ones for the other polymers. Although the non-attractive segments lie in the middle of chain, the desorption of attractive segments in two ends of chain causes the favorite form of short tail adsorption. The other peak of $B_{10}A_{10}B_{10}$, also for $(A_{1/3}B_{2/3})_{30}$ and A_{30}^{homo}, appears at $n = 29$, corresponding to the case when only one segment is adsorbed, which would become smaller for larger energy comparing with the second peaks at $n = 1$ as shows in figure 3(b). Obviously, the latter peak is attributed to the contribution of segment B. Both peak values increase as $\tilde{\varepsilon}_{\mathrm{Aa}}$ increases, however characteristic peaks increase faster.

Interestingly, the size distributions of tails for random copolymer $(A_{1/3}B_{2/3})_{30}$ and homopolymer A_{30}^{homo} are almost the same, but different from the other copolymers completely. Therefore, the size distribution of tails is dependent on the sequence of attractive segments in polymer chains, and that of random copolymers could be described by an equivalent homopolymer.

The size distributions of trains are shown in figure 4(a),(b). The size distributions of trains for all the samples have only one peaks at $n = 2$ when the adsorption energy is smaller, and the value is almost the same as shown in figure 4(a). However, when $\tilde{\varepsilon}_{\mathrm{Aa}}$ becomes higher, the size distributions of trains for three samples form the second peaks, at $n = 5$ for $A_5B_{20}A_5$, at $n = 10$ for $A_{10}B_{20}$ and $B_{10}A_{10}B_{10}$ which just equals to the length of attractive block A, as shown in figure 4(b). With the increase of *n*, the distribution curve decreases faster for the former than for the latter. It means that all attractive segments would be adsorbed on the surfaces if only the adsorption energy is strong enough. However, the second peak of $A_{10}B_{20}$ is higher than that of $B_{10}A_{10}B_{10}$ because the middle copolymer $B_{10}A_{10}B_{10}$ has two non-attractive blocks in the ends of chain which tend to make middle block A extending to the bulk. Accordingly, we can make the conclusion that the size distribution of trains is determined by the attractive block A. The first peak always appears at $n = 2$, the second peak appears at the length of a block of attractive segments; but whether the second peak of train configuration appears or not is determined by the interaction between segment and surface. If the length is shorter, the emergence of the second peak of trains only needs a small energy. Increasing the length of trains is a natural result of strengthening the total adsorption energy. The most favorable longest length of *n* corresponds to the length of continuous attractive block A. It means the stronger attraction favors longer train. In any way, $(A_{1/3}B_{2/3})_{30}$ and A_{30}^{homo} just have one peak at $n = 2$ the value of which increases with the adsorption energy. It is because the distribution of attractive segments in $(A_{1/3}B_{2/3})_{30}$ chain is random, no continuous block of segment A is dominant, and the second peak will not appear. For homopolymer A_{30}^{homo}, which is composed of attractive segments only, a second peak has not been found in previous works. Again, we found that the size distributions of trains for $(A_{1/3}B_{2/3})_{30}$ and A_{30}^{homo} are similar.

Downloaded At: 17:46 14 January 2011

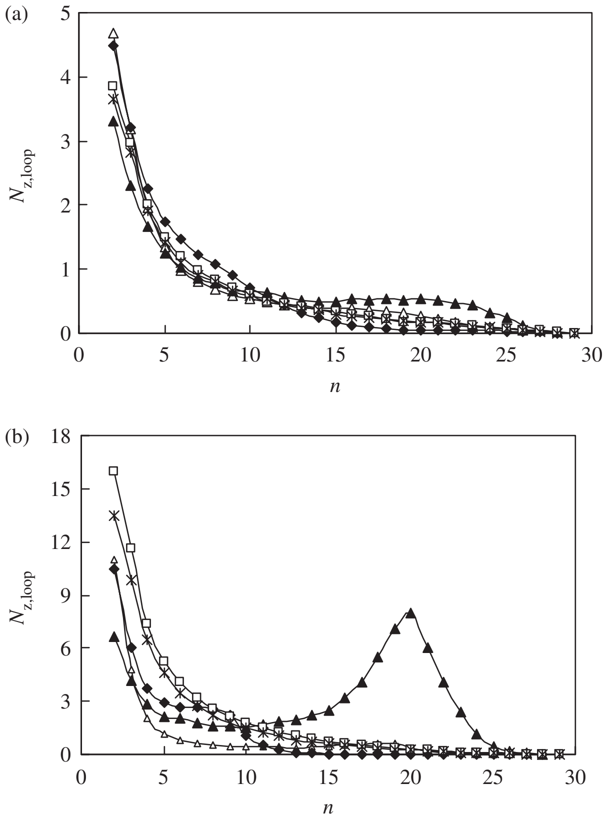

Figure 5. Size distributions of loop configurations for five systems with $\Phi_c = 0.0048$ when $\tilde{\varepsilon}_a^{\text{molecule}} = 0.133$ (a) and $\tilde{\varepsilon}_a^{\text{molecule}} = 0.4$ (b). Legends are as in figure 1.

Downloaded At: 17:46 14 January 2011

The size distributions of loops are shown in figure 5(a),(b). For all polymers, just one maximum appears at $n = 2$ when $\tilde{\varepsilon}_{\text{Aa}}$ is smaller, which implies the smallest loop with two segments is most likely in the adsorption layers. The number of loops decreases monotonously with the increase of the size n. Comparatively, a plateau is observed for $A_5B_{20}A_5$ because the block of non-attractive in the middle is the longest among all polymers, which is favorable to form larger loops. However, when $\tilde{\varepsilon}_{\text{Aa}}$ is higher, only for $A_5B_{20}A_5$, there becomes another peak at $n = 20$ which just equals to the length of block B as shown in figure 5(b), indicating more chance to form bigger loop configuration when both two-terminals are attracted to the surface as expected. The latter means the two attractive blocks are both adsorbed onto the surface at the same time. The size distribution of loops could be bimodal for end-adsorbed copolymer when the energy is larger. The length of the middle non-attractive block determines the location of the second peak. However, it is similar to the case of trains that only one maximum is observed for $(A_{1/3}B_{2/3})_{30}$ and A_{30}^{homo} in loops. Also the size distributions of loops for them are the same roughly.

It is found both peak values increase as $\tilde{\varepsilon}_{\text{Aa}}$ increases. When the adsorption energy is strong enough, the size distributions of various configurations of all adsorbed copolymers are characteristic except for random copolymer which could be seen from figures 3(a), 4(a) and 5(a). The tails are more appearing at n that equals to the length of non-attractive block in the end of chains, the trains tend to appear at n which equal to the length of attractive block A. With the adsorption energy we adopt, only end-adsorbed copolymer forms a peak at n equals to the length of non-attractive block in the middle of chains.

The size distributions of homopolymer and random copolymer are monodisperse as compared with the other polymers, it is because homopolymer is composed of one kind segment which has the same chance to be adsorbed on the surface. For random copolymer, the chain sequence of polymers is random that two kinds of segments have same probability of arrangement in a chain, so the adsorption behavior of random copolymers could be imitated by an equivalent homopolymer.

It has been known that the adsorption of random copolymers differs greatly from that of other copolymers, but acting like homopolymers. The latter usually adsorbs at several points along the chain with various configurations such as train, loop, and tail. A block copolymer usually has some longer blocks adsorbed on the surface in a rather flat conformation, whereas the other blocks have a lower or no surface affinity extend into the solution. Therefore, it is reasonable to expect that the attractive segment A plays an important role in trains and loops, while the non-attractive segment B constitutes the main part of tails.

3.3 The surface coverage

Figure 6 illustrates the surface coverage vs. different bulk concentration for all polymers with $\tilde{\varepsilon}_{\text{Aa}} = 1.2$, where for (a) total segment, (b) A segment and (c) B segment. From simulations, we found that all the surface coverage for five samples increased monotonously with the increase of bulk concentration when the reduced adsorption energy was relatively large. However, the relative position is rather different from each other. The upper one is for $A_{10}B_{20}$, the middle for $B_{10}A_{10}B_{10}$ and $A_5B_{20}A_5$, and the lower for $(A_{1/3}B_{2/3})_{30}$ and A_{30}^{homo}, respectively.

In fact, the density of segment A in the first layer is exactly the surface coverage of segment A. As shown in figure 6(b), the surface coverage of segment A (θ_A) is ordered in value from $A_{10}B_{20}$, $B_{20}A_{10}B_{20}$, $A_5B_{20}A_5$, $(A_{1/3}B_{2/3})_{30}$ to A_{30}^{homo}. In figure 1(a), it shows that $\tilde{\varepsilon}_{\text{Aa}}$, as well as $\tilde{\varepsilon}_a^{\text{polymer}}$, of different copolymers is the same, but the surface coverage of segment A is distinguishing due to the chain structure of various copolymers. The surface coverage of segment B (θ_B) was also studied in figure 6(c), this order would tend to be reverse. θ_B for $B_{10}A_{10}B_{10}$ and $A_5B_{20}A_5$, which increases more mildly, is nearly the same. Despite the amount is small, it contributes to the surface coverage and influences the further adsorption of copolymer chains. θ_B for $(A_{1/3}B_{2/3})_{30}$ is much higher than that for others because the arrangement of segment A and B in a chain is random. Although the segment B is non-attractive, the connectivity between block A and block B makes it possible that segment B may accidentally be located on the surface, i.e. be adsorbed.

Downloaded At: 17:46 14 January 2011

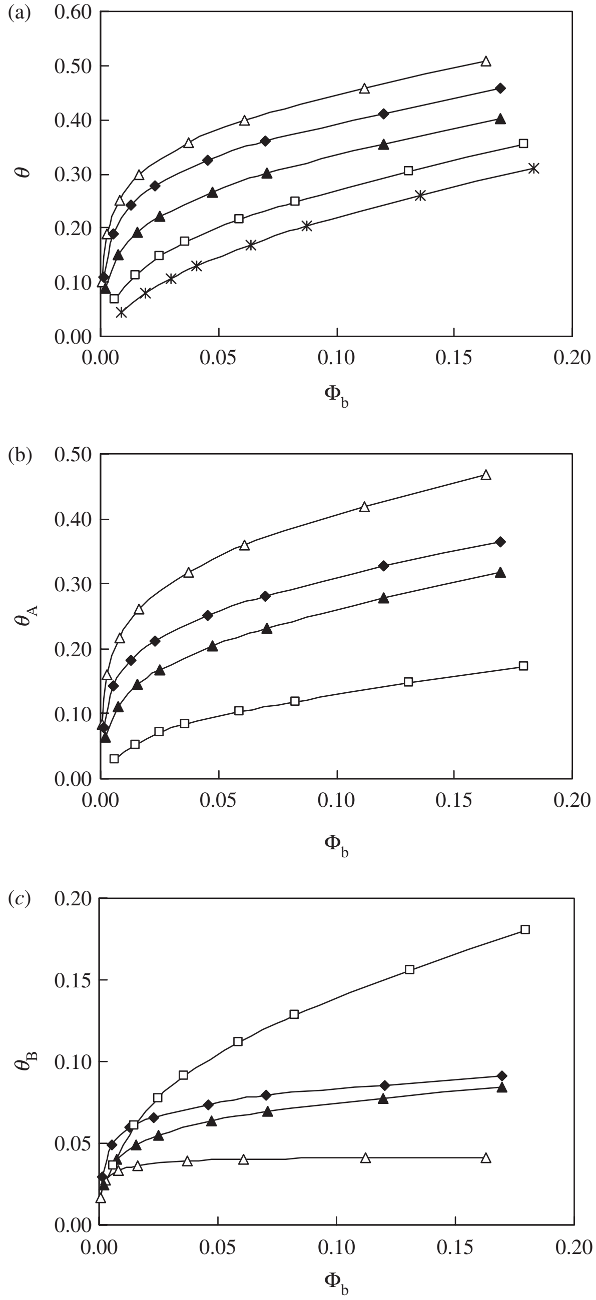

Figure 6. Surface coverage in different bulk concentration for five systems when $\varepsilon_a^{molecule} = 0.4$. (a) Total segment, (b) A segment, (c) B segment. Legends are as in figure 1.

The value of surface coverage depends on the relative number of attractive segments and non-attractive segments. For series of a rather shorter non-attractive block and longer attractive block, the difference of surface coverage between each other is not so large and can be neglected. It means that when non-attractive segment block is much shorter than attractive one, the influence of sequence of copolymer on surface coverage is not great.

3.4 The adsorption amount

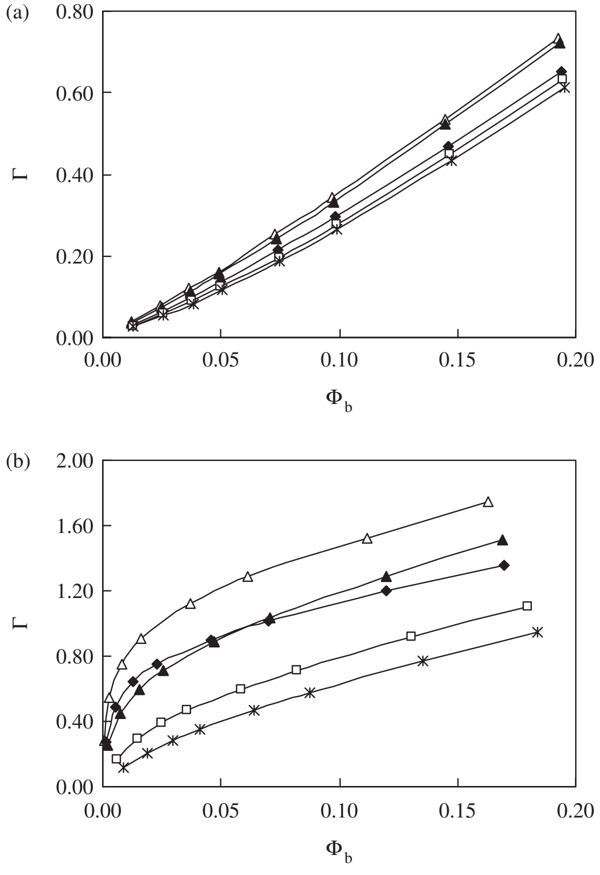

Figure 7. Adsorption isotherms for five systems at $\varepsilon_a^{molecule} = 0.133$ (a) and $\varepsilon_a^{molecule} = 0.4$ (b). Legends are as in figure 1.

The adsorption amount (expressed in equivalent lattice layers) is determined by those molecules having at least one segment in the lattice layer directly adjacent to the surface. Adsorption isotherms for all copolymers are plotted in figure 7. It increases as the bulk concentration increases for all polymer systems. The adsorbed amount is ordered in value from $A_{10}B_{20}$ and $B_{10}A_{10}B_{10}$, $A_5B_{20}A_5$, $(A_{1/3}B_{2/3})_{30}$ to A_{30}^{homo} in figure 7(a). However, the difference between $A_{10}B_{20}$ and $A_5B_{20}A_5$ is very small when $\tilde{\varepsilon}_{Aa} = 1.2$. The order will not change in principle as $\tilde{\varepsilon}_{Aa}$ increases, except the adsorbed amount of $B_{10}A_{10}B_{10}$ is greater than that of $A_5B_{20}A_5$ when $\phi_b \leq 0.05$, and the former is even lower than the latter as ϕ_b further increases.

When $\hat{\varepsilon}_a^{eff}$ is small, the adsorption mount Γ of homopolymer increases almost linearly with the bulk concentration as shown in figure 7(a), which is the same as $(A_{1/3}B_{2/3})_{30}$. As ε_a^{eff} increases, resulting in higher total adsorption energy and higher adsorption amount, the curves gradually become convex, and the dependence on the concentration is weaker at higher bulk concentrations as shown in figure 7(b). Even though it has deviations between $(A_{1/3}B_{2/3})_{30}$ and A_{30}^{homo}, the adsorption amount of random copolymer is always a little higher than that of homopolymer.

3.5 The adsorption layer thickness

The adsorption layer thickness vs. bulk concentration for five systems with different adsorption energy is depicted in

Downloaded At: 17:46 14 January 2011

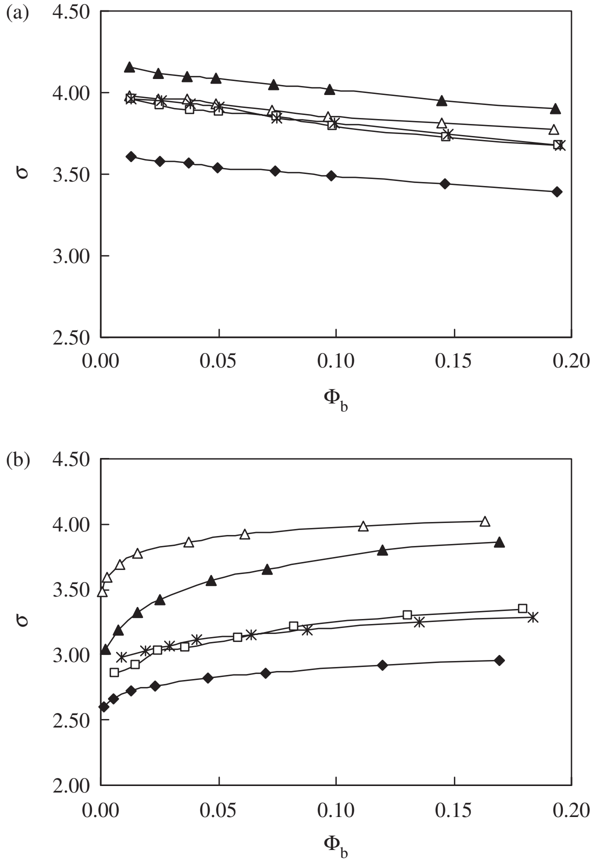

Figure 8. Absorption layer thickness with different bulk concentration for five systems at $\varepsilon_a^{\text{molecule}} = 0.133$ (a) and $\varepsilon_a^{\text{molecule}} = 0.4$ (b). Legends are as in figure 1.

figure 8(a),(b). The effect of adsorption energy on adsorption layer thickness shows different trend in different region. When $\tilde{\varepsilon}_{\text{Aa}}$ is smaller, the adsorbed layer thickness σ for all polymers decreases linearly with the increase of bulk concentration. The thickness is the largest for $A_5B_{20}A_5$ and the smallest for $B_{10}A_{10}B_{10}$, while the others seem to almost be similar. There are more loops $n = 25$ for $A_5B_{20}A_5$, but the other end of two-terminal copolymer is absorbed when $\tilde{\varepsilon}_{\text{Aa}}$ becomes larger. However, σ for all the polymers increases, with the increasing of bulk concentration when $\tilde{\varepsilon}_{\text{Aa}} = 1.2$. The adsorbed layer thickness exhibits firstly a little raise and then increases slightly as bulk concentration increases, and also the relative position of thickness is something different. In this case, the largest thickness is for $A_{10}B_{20}$ because it forms bigger tails which can be seen from figure 3(a),(b). The RMS layer thickness of $(A_{1/3}B_{2/3})_{30}$ and A_{30}^{homo} is located in between that of $A_5B_{20}A_5$, $A_{10}B_{10}$ and $B_{10}A_{10}B_{10}$. Another result is that the increase of layer thickness for $(A_{1/3}B_{2/3})_{30}$ and A_{30}^{homo} with the bulk concentration is the same.

The higher the adsorption energy, the smaller the layer thickness is, because of the tighter adsorption. The results show that the adsorption layer thickness depends on the sequence of copolymer. It implies that the number and size of tails together play a more important role in determining the thickness of adsorption layer.

4. Conclusion

MC simulations on a cubic lattice have been performed to illustrate the surface adsorption behavior of polymers. A series of systematic comparisons between random copolymer and other copolymers are provided in the microstructure and macrostructure information of adsorption layers. The effects of block and interaction parameters on adsorption behavior have been investigated. The results of simulation show that the position of attractive block in a copolymer chain affects the adsorption behavior.

The adsorption behavior of random copolymers, which acts like homopolymer, is remarkably different from that of other copolymers. For all polymers, the size distribution of various configurations depends on the sequence of copolymers and the interaction energy between segment and surface. Where the position and intensity of characteristic peak appears is determined by the length of attractive block and non-attractive block.

The density profiles of block copolymers show a dense A layer on the surface and B tails dangling into the bulk, whereas random copolymers show a monotonous homopolymer-like segment density profiles. At a constant fraction of A segments, the adsorbed amount increases with increasing bulk concentration while the adsorption layer thickness is dependent on the adsorption energy. Diblock copolymer has the highest adsorbed amount as random copolymers and homopolymers give the smallest surface coverage and the smallest adsorbed amount. The adsorption of random copolymers is usually stronger than that of a homopolymer with equal length and consisting of the same type of adsorbing segments. Therefore homopolymer always gives the smallest surface coverage as well as the adsorbed amount.

In conclusion, the sequence of polymer chains, i.e. molecular structure, is the most important factor in affecting adsorption properties at the same composition and interaction between segment and surface. However, the adsorption behavior of random copolymer is always similar to that of homopolymer, which indicates an equivalent homopolymer could take the place of random copolymer.

Acknowledgements

This work is supported by the National Natural Science Foundation of China (Projects no. 20476025,20676030, 20490204), the Doctoral Research Foundation sponsored by the Ministry of Education of China (Project no. 20050251004), and Shanghai Municipal Science and Technology Commission of China (no. 05DJ14002).

References

[1] L. Dai, C. Toprakcioglu. End-adsorbed triblock copolymer chains at the liquid–solid interface: bridging effects in a good solvent. *Macromolecules*, **25**, 6000 (1992).
[2] L. Dai, C. Toprakcioglu, G. Hadziioannou. Conformational transitions of end-adsorbed copolymer chains at the liquid/solid interface. *Macromolecules*, **28**, 5512 (1995).

[3] J.R. Dorgan, M. Stamm, C. Toprakcioglu, R. Jérôme, L.J. Fetters. End-attaching copolymer adsorption: kinetics and effects of chain architecture. *Macromolecules*, **26**, 5321 (1993).

[4] J.B. Vieira, Z.X. Li, R.K. Thomas. Adsorption of triblock copolymers of ethylene oxide and propylene oxide at the air/water interface: the surface excess. *J. Phys. Chem. B*, **106**, 5400 (2002).

[5] S.T. Milner, T.A. Witten. Bridging attraction by telechelic polymers. *Macromolecules*, **25**, 5495 (1992).

[6] C.M. Wijmans, F.A.M. Leermakers, G.J. Fleer. Multiblock copolymers and colloidal stability. *J. Colloid Interface Sci.*, **167**, 124 (1994).

[7] M. Björling, P. Stilbs. Using end-confined chains to model end-adsorbing, triblock copolymers: 1. Analytical approach. *Macromolecules*, **31**, 9033 (1998).

[8] Y. Zhan, W.L. Mattice, D.H. Napper. Monte Carlo simulation of the adsorption of diblock copolymers from a nonselective solvent. I. Adsorption kinetics and adsorption isotherms. *J. Chem. Phys.*, **98**, 7502 (1993).

[9] Y. Zhan, W.L. Mattice, D.H. Napper. Monte Carlo simulation of the adsorption of diblock copolymers from a nonselective solvent. II. Structure of adsorbed layer. *J. Chem. Phys.*, **98**, 7508 (1993).

[10] T.C. Clancy, S.E. Webber. Controlling adsorption of polymers at polymer-modified surfaces. *Macromolecules*, **30**, 1340 (1997).

[11] Y. Wang, Y. Li, W.L. Mattice. Simulation of the adsorption of symmetric diblock copolymers at the interface of the two monomeric homopolymers. *J. Chem. Phys.*, **98**, 9881 (1993).

[12] Y. Wang, Y. Li, W.L. Mattice. Simulation of adsorption of unsymmetric diblock copolymers at the interface between the two monomeric homopolymers. *J. Chem. Phys.*, **99**, 4068 (1993).

[13] Y. Wang, I. Teraoka. Structures and thermodynamics of nondilute polymer solutions confined between parallel plates. *Macromolecules*, **33**, 3478 (2000).

[14] S.H. Kim, W.H. Jo. A Monte Carlo simulation of polymer/polymer interface in the presence of block copolymer. I. Effect of the chain length of block copolymer and interaction energy. *J. Chem. Phys.*, **110**, 12193 (1999).

[15] T. Geisinger, M. Muller, K. Binder. Symmetric diblock copolymers in thin film. I. Phase stability in self-consistent field calculations and Monte Carlo simulations. *J. Chem. Phys.*, **111**, 5241 (1999).

[16] T. Geisinger, M. Muller, K. Binder. Symmetric diblock copolymers in thin film. II. Comparison of profiles between self-consistent field calculation and Monte Carlo simulations. *J. Chem. Phys.*, **111**, 5251 (1999).

[17] S. Misra, W.L. Mattice. Telechelic polymers between two impenetrable adsorbing surfaces. *Macromolecules*, **27**, 2058 (1994).

[18] M. Nguyen-Misra, S. Misra, W.L. Mattice. Bridging by end-adsorbed triblock copolymers. *Macromolecules*, **29**, 1407 (1996).

[19] A.C. Balazs, S. Lewandowski. Models for the surface adsorption of triblock copolymers. *Macromolecules*, **23**, 839 (1990).

[20] T. Haliloglu, D.C. Stevenson, W.L. Mattice. Monte Carlo simulation of the adsorption from a nonselective solvent of symmetric triblock copolymers with sticky end blocks. *J. Chem. Phys.*, **106**, 3365 (1997).

[21] T. Cosgrove, N.A. Finch, J.R.P. Webster. Monte Carlo simulations of adsorbed random copolymers. *Macromolecules*, **23**, 3353 (1990).

[22] S. Chidambaram, M.D. Dadmun. A Monte Carlo study of the effect of polymer rigidity on adsorption behaviour. *Comput. Theor. Polym. Sci.*, **9**, 47 (1999).

[23] J.W. Jiang, H.L. Liu, Y. Hu. Lattice Monte Carlo simulation of polymer adsorption at an interface 1. Monodisperse polymer. *Macromol. Theory Simul.*, **7**, 105 (1998).

[24] J.W. Jiang, H.L. Liu, Y. Hu. Lattice Monte Carlo simulation of polymer adsorption at an interface 2. Polydisperse polymer. *Macromol. Theory Simul.*, **7**, 113 (1998).

[25] T. Chen, H.L. Liu, Y. Hu. Monte Carlo simulation for the adsorption of diblock copolymers I. In nonselective solvent. *J. Chem. Phys.*, **114**, 5937 (2001).

[26] C.J. Peng, J.K. Li, H.L. Liu, Y. Hu. Adsorption behavior of asymmetrical triblock copolymers at the solid–liquid interface by Monte Carlo simulation. *Macromol. Theory Simul.*, **13**, 711 (2004).

[27] J.K. Li, C.J. Peng, H.L. Liu, Y. Hu. Monte Carlo simulation for the adsorption of symmetric triblock copolymers I. Configuration distribution and density profiles of adsorbed chains. *Eur. Polym. J.*, **41**, 627 (2005).

[28] C.J. Peng, J.K. Li, H.L. Liu, Y. Hu. Monte Carlo simulation for the adsorption of symmetric triblock copolymers II. Adsorption layer information. *Eur. Polym. J.*, **41**, 637 (2005).

[29] M.N. Rosenbluth, A.W. Rosenbluth. Monte Carlo calculations of the average extension of molecular chains. *J. Chem. Phys.*, **23**, 356 (1955).

[30] P.H. Verdier, W.H. Stockmayer. Monte Carlo calculations on the dynamics of polymers in dilute solution. *J. Chem. Phys.*, **36**, 227 (1962).

[31] J.M.H.M. Scheutjens, G.J. Fleer. Interaction between two adsorbed polymer layers. *Macromolecules*, **18**, 1882 (1985).

Downloaded At: 17:46 14 January 2011